

This article was downloaded by:

On: 22 January 2011

Access details: *Access Details: Free Access*

Publisher *Taylor & Francis*

Informa Ltd Registered in England and Wales Registered Number: 1072954 Registered office: Mortimer House, 37-41 Mortimer Street, London W1T 3JH, UK



The Journal of Adhesion

Publication details, including instructions for authors and subscription information:

<http://www.informaworld.com/smpp/title~content=t713453635>

Fatigue Performance of Two Structural Adhesives

Jeenarainsingh Luckyram^a; Alan E. Vardy^a

^a Wolf son Bridge Research Unit, University of Dundee, Dundee, U. K.

To cite this Article Luckyram, Jeenarainsingh and Vardy, Alan E.(1988) 'Fatigue Performance of Two Structural Adhesives', *The Journal of Adhesion*, 26: 4, 273 – 291

To link to this Article: DOI: 10.1080/00218468808071291

URL: <http://dx.doi.org/10.1080/00218468808071291>

PLEASE SCROLL DOWN FOR ARTICLE

Full terms and conditions of use: <http://www.informaworld.com/terms-and-conditions-of-access.pdf>

This article may be used for research, teaching and private study purposes. Any substantial or systematic reproduction, re-distribution, re-selling, loan or sub-licensing, systematic supply or distribution in any form to anyone is expressly forbidden.

The publisher does not give any warranty express or implied or make any representation that the contents will be complete or accurate or up to date. The accuracy of any instructions, formulae and drug doses should be independently verified with primary sources. The publisher shall not be liable for any loss, actions, claims, proceedings, demand or costs or damages whatsoever or howsoever caused arising directly or indirectly in connection with or arising out of the use of this material.

Fatigue Performance of Two Structural Adhesives

JEENARAINSINGH LUCKYRAM and ALAN E. VARDY

Wolfson Bridge Research Unit, University of Dundee, Dundee DD1 4HN, U.K.

(Received November 21, 1987; in final form April 19, 1988)

The fatigue performance of two toughened epoxy adhesives suitable for use in heavy structural engineering is assessed using a purpose-built fatigue rig. One adhesive is of the single-part, hot-cure type and the other is a two-part, cold-cure system. It is found that the single-part adhesive performs better than the two-part adhesive in fatigue even though the latter has the higher fracture toughness. Crack growth rates in both adhesives are found to satisfy the Paris Law as closely as any other crack growth model, and no dependence is found on the frequency of load cycling in the range studied (0.5 Hz–5 Hz). The fatigue performance of both adhesives is very promising for their likely uses in large-scale structures.

KEY WORDS Fatigue; epoxy adhesives; fracture toughness; fatigue machine; frequency dependent crack propagation; cyclic fracture.

I INTRODUCTION

Adhesives have been used extensively in the aircraft and ground vehicle industries for many years. They have proved to be economical as well as providing the means to create strong joints with clear lines. In contrast, they have been used relatively little in heavy structural engineering except in the production of laminated timber beams. Some examples exist where steel plates have been bonded externally to concrete beams,^{1,2} but the authors are unaware of any instances of bonded steel/steel joints in new construction. However, Albrecht³ has shown that the fatigue life of adhesively bonded cover plates on the tension flange of a steel girder can be hugely greater than that of welded cover plates provided that the plate ends are bolted to prevent debonding. Also, Martin⁴ has demonstrated a

similar superiority of adhesively bonded web stiffeners (his work will shortly be offered for wider publication).

An important reason for the scarcity of uses of adhesives in heavy structural engineering is a lack of information about the long term properties of appropriate types of adhesive in adverse environmental conditions and stress regimes. This has prompted an extensive programme of experimental and theoretical work on adhesives in the Wolfson Bridge Research Unit at the University of Dundee. The desirable characteristics of potentially useful adhesives are now known quite well,⁵ as are the mechanical properties of the various chemical formulations.⁶

Of the many types of adhesives evaluated in the Unit, toughened epoxies stand out as the most promising for structural uses, provided that appropriate measures are taken to prevent moisture uptake (e.g. painting exposed edges of the bonds). Toughened adhesives have relatively high fracture toughnesses and, when applied to well-prepared surfaces, enable the creation of reliable joints with good peel strengths. Also, laboratory tests have shown these types of adhesive to have excellent fatigue properties. However, the emphasis hitherto has been on the "safe-life" approach to fatigue in which endurance limits are established for particular joint configurations. There is some danger in extrapolating the results of such tests to new joint configurations or even to the same joint loaded differently.

Material scientists tend to prefer designs to be based on the "fail-safe" approach in which crack growth rates are predicted, rather than endurance limits. With this approach, crack growth is assumed to be caused by stress fluctuations close to the crack tip, and experimental results using one configuration can be used to predict behaviour in other configurations. This is especially valuable when assessing the future life of structures with known cracks and when predicting the effects of remedial or supplementary strengthening.

Objectives

The main purposes of the present paper are:

- 1) to present data on the fatigue performance of adhesives characteristic of those likely to be used for bonding steel to itself or to concrete, and

2) to establish a suitable form in which to present these data, taking account of mean stress levels as well as stress ranges and fatigue cycling rates.

The two adhesives selected for detailed study are designated numbers 16 and 21 within the Wolfson Bridge Research Unit. Both are rubber-toughened epoxies which have performed well under static and cyclic loads after exposure to a wide range of environments (*e.g.* alternate wetting and drying, temperature cycling). Their principal structural properties after hardening are listed in Table I. These values have been obtained from tensile tests on several 3 mm-thick dumbbell specimens using an Instron testing machine.

TABLE I
Properties of hardened adhesives

Adhesive number	Young's modulus MPa	Poisson's ratio	Ultimate strain	Ultimate stress, MPa
16	6600	0.38	0.014	49.6
21	2200	0.42	0.065	29.4

Adhesive No 16 is a one-part, heat-curing adhesive that is particularly suitable for bonding steel to itself. In a typical joint, the adhesive layer is about 1 mm thick and curing can take place at temperatures between 90°C and 200°C. At 150°C the curing time is 2 hours. The adhesive is silver grey in colour and contains a coarse metallic filler. At room temperature it is a soft, non-flowing paste.

Adhesive No 21 is a two-part, cold-cure adhesive well suited to bonding steel to concrete, but also suitable for bonding steel to itself. Typically the adhesive thickness in a joint is about 1 mm. The joint must be formed within 90 minutes of mixing and left to cure for 24 hours at room temperature. More rapid curing is possible at higher temperatures (up to 100°C). The resin is a viscous opalescent paste incorporating a liquid rubber modifier. The hardener is a straw-coloured, liquid, aliphatic polyamine. The hardener and the resin must be thoroughly mixed in the ratio of 44:100 by weight and care must be taken to minimise the entrapment of air bubbles which inevitably create stress concentrations in the finished product.

II CRACK GROWTH MODELS

Numerous fatigue crack growth "laws" have been proposed in the past. These models were mainly developed from work on metals and have been reviewed by Hoepfner and Krupp.⁷ The most widely used crack growth model, due to Paris and Erdogan,⁸ can be expressed as

$$\frac{da}{dN} = A_1(\Delta K)^{B_1} \quad (1)$$

where a is the crack length, N the number of cycles, K the stress intensity factor and A_1 and B_1 are material constants. Equation (1) is often alternatively expressed in terms of the strain release rate, G^{9-13} as

$$\frac{da}{dN} = A_2(\Delta G)^{B_2} \quad (2)$$

The Paris Law has been used successfully, to describe crack growth in various materials which satisfy the assumptions of linear elastic fracture mechanics (LEFM). Under elastic-plastic and gross yielding conditions, da/dN can be correlated to the range of the J -integral, ΔJ^{13-15} or to the range of crack tip opening displacement, $\Delta CTOD$.^{13,15}

Forman *et al.*¹⁶ have shown that R , the ratio of the minimum and maximum stresses during cycling, is an important parameter in crack propagation close to the onset of fast fracture because K_{\max} , the maximum stress intensity factor, approaches K_c , the fracture toughness of the material. The stress ratio is included in Forman's formula:

$$\frac{da}{dN} = \frac{A_3(\Delta K)^{B_3}}{K_c(1-R) - \Delta K} \quad (3)$$

where A_3 and B_3 are material constants.

Forman's equation has been successfully used to characterise the fatigue performance of various metals¹⁷ but Radon *et al.*¹³ found that it does not apply to polymers. They argued that apart from the range of stress intensity factor, ΔK , and the mean stress intensity factor, K_{mean} , the maximum stress intensity factor, K_{\max} , also has an

influence on fatigue crack propagation. To allow for this, they proposed the use of the expression

$$\frac{da}{dN} = A_4 \lambda^{B_4} \quad (4)$$

where

$$\lambda = (K_{\max}^2 - K_{\min}^2) = 2\Delta K \cdot K_{\text{mean}}$$

A_4 and B_4 are material constants.

Equation (4) has shown good correlation for fatigue data on metals¹³ and polymers.¹⁸

In another attempt to formulate a unified approach to fatigue crack propagation for metals and non-metals, Woo and Chow¹⁹ suggested the following:

$$\frac{da}{dN} = \frac{A_5(\Delta G)^{B_5}}{(G_c - G_{\max})} \quad (5)$$

where G_c is the critical strain energy release rate and G_{\max} the maximum strain energy release rate. Equation (5) indirectly takes into account the effect of mean stress and was shown to give superior correlation to the Paris Law and the Forman's formula for data on aluminium alloys and PMMA.¹⁹

Elber²⁰ observed that fatigue cracks can close during the unloading phase of each cycle even when the applied load remote from the crack tip remains tensile. This led him to propose the use of an effective stress intensity factor range, ΔK_{eff} , defined by

$$K_{\text{eff}} = (0.5 + 0.4R) \Delta K \quad (6)$$

in place of ΔK in the Paris Law (Eq. (1)) leading to

$$\frac{da}{dN} = A_6 [(0.5 + 0.4R) \Delta K]^{B_6} \quad (7)$$

This has been successfully applied to fatigue crack growth in metals²⁰ and structural adhesives.¹⁰

None of the above formulae takes into account the frequency of load cycling. Indeed, numerous experiments have shown that various metals exhibit negligible dependence of crack growth rates on frequency. However, polymers tend to be less well behaved,

some showing increasing fatigue crack propagation rates at higher frequencies and others showing decreasing rates at higher frequencies.²¹ Marceau *et al.*⁹ reported the latter behaviour for an unspecified adhesive.

It is noteworthy that fatigue testing in laboratories tends to be carried out at relatively high frequencies, typically greater than 1 Hz and often greater than 10 Hz. This has the advantage of enabling experiments to be completed relatively quickly, but the disadvantage of missing certain frequencies of relevance in engineering practice. In civil engineering, diurnal phenomena can be of considerable interest, as can be annual fluctuations and even much rarer events—occasional extreme loads, for instance. The experiments reported herein have been carried out at frequencies of the order of 1 Hz and so do not allow sufficient time for the effects of creep to produce strong non-linearities. This limitation will need to be rectified before the widespread use of adhesives can be contemplated in civil engineering.

III COMPACT TENSION SPECIMENS

The Compact Tension Specimen recommended in the ASTM standard E647²² for Mode I fracture investigations is used throughout this study. The dimensions of the specimen are shown in Figure 1 and Eq. (8) is used for the computation of stress intensity factor ranges.

$$\Delta K = \frac{\Delta P}{BW^{1/2}} \frac{(2 + \alpha)}{(1 - \alpha)^{3/2}} \{0.886 + 4.64\alpha - 13.32\alpha^2 + 14.72\alpha^3 - 5.60\alpha^4\} \quad (8)$$

where $\alpha = a/W$ and B and W are dimensions shown in Figure 1. The expression is valid for $a/W \geq 0.2$.

The laboratory specimens were cast in a specially designed steel mould which creates the notch and the support holes directly. The wet adhesive (mixed in the case of adhesive 21) was poured slowly into the mould and tamped to minimise the entrapment of air bubbles. A cover plate clamped to the top of the mould ensured the production of smooth specimens of the correct size.

Adhesive 16 was placed in a pre-heated, air-circulating oven at 150°C for 2 hours and kept at room temperature for a further 24

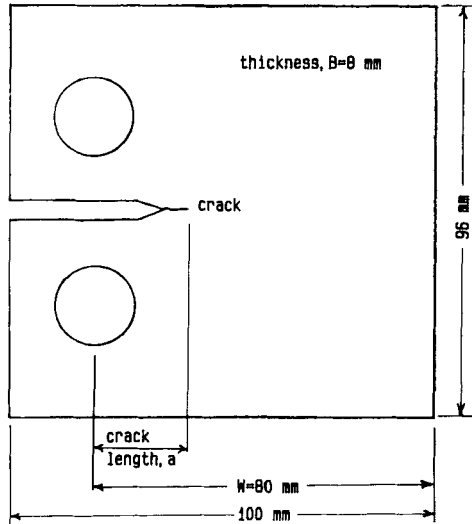


FIGURE 1 All-adhesive Compact Tension Specimen.

hours before demoulding. Adhesive 21 was simply kept at 20°C for 24 hours before demoulding. Both types were subsequently stored at 20°C until use.

IV EXPERIMENTAL PROCEDURE

Most fatigue tests are carried out in servo-hydraulic machines which are typically designed to produce the relatively high loads necessary for testing metal specimens. Such machines are not necessarily well suited to testing polymers where the loads to be applied to the specimen can be small in comparison with the forces required to accelerate the moving parts of the machine. A second disadvantage of most machines is that only one specimen can be tested at a time, thus leading either to extended testing periods or to extensive financial outlay.

To overcome these limitations of servo-hydraulic machines, a simple mechanical rig has been fabricated. The main features of the rig, described in detail by Luckyram, Harvey and Vardy²³ are illustrated in Figure 2. This shows only a single specimen, but the

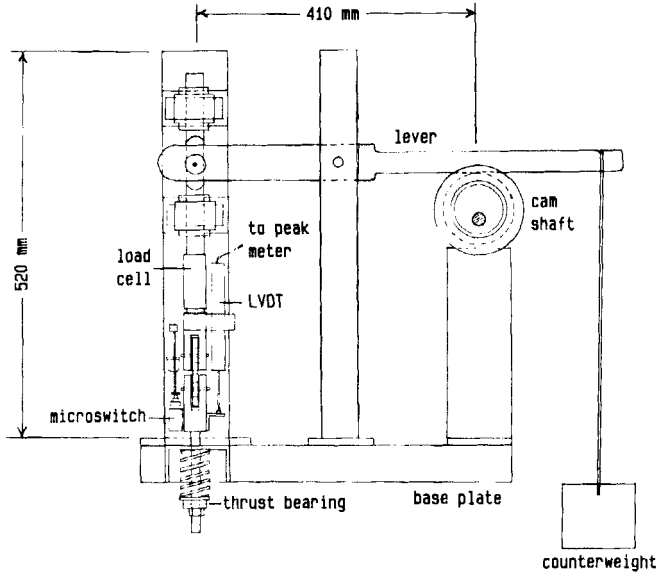


FIGURE 2 New fatigue testing machine: end elevation.

actual rig has four such specimens on a common shaft and could be extended to accommodate more specimens. Each specimen is mounted between a lever and a spring. The initial load is induced by an adjusting nut beneath the spring, and the cyclic load is applied by tilting the lever by means of a cam on the main shaft. Different stress ranges are achieved with a particular cam by using springs of different stiffnesses.

The number of cycles is recorded by a meter activated at the spring (so that counting ceases when the specimen fails), the relative displacement of the loading arms is measured with an LVDT, and the load is monitored by a load cell mounted between the lever and the specimen. The latter two measurements enable the compliance to be determined directly.

The crack length is measured with the aid of a travelling microscope mounted on a platform fixed to the base of the machine. In practice, this is found to be a reliable and simple procedure that is far less time consuming than was initially expected. Nevertheless, the need to record the crack length manually has the disadvantage

of requiring the operator to be present at any time of day or night when rapid crack propagation is expected. The possibility of using electrical methods of monitoring crack lengths would merit serious consideration in an establishment where cheap, reliable labour is not available.

A second disadvantage of the current set-up is that the mean stress level in the specimen reduces slightly as the crack length increases. This is counteracted by adjusting the nut beneath the spring occasionally. The effect is only slight and it does not seem worthwhile to automate the procedure by, say, activating a stepper motor in response to the load detected by the load cell.

In a typical test, a small crack is formed with a sharp blade at the end of the notch in the compact tension specimen. The specimen is then mounted in the machine and loaded cyclically until the crack begins to grow. The test is deemed to begin after the crack has grown by a measurable amount, indicating that conditions near the tip are representative of a fatigue crack. The number of cycles during subsequent crack growth is recorded at frequent intervals. This preliminary stage of the experiment can be quite lengthy in some cases. It typically lasts one or two days for adhesive 21 and a few weeks for adhesive 16 though the mean stress level is increased by up to 40% so that K_{\max} approaches K_c .

After the end of the test, the two halves of each specimen can be inspected visually to determine the crack length immediately before ultimate failure. The value is then used to deduce the fracture toughness of the particular specimen—which appears explicitly in Woo and Chow's crack growth rate formula (Eq. (5)). In practice, this is easily done in the case of adhesive 16 because the boundary between the regions of fatigue crack propagation and fast fracture is easily defined. It is not straightforward with adhesive 21, however, because the boundary is much less clear. It follows that the value of G_c is not known with high accuracy for adhesive 21.

V FATIGUE PERFORMANCE

The two adhesives behaved quite differently in the fatigue tests with adhesive 16 exhibiting a markedly superior performance. The initiation of a fatigue crack is more difficult and the rate of growth of the crack, once formed, is smaller than in adhesive 21.

TABLE II
Fracture toughness of adhesives

Adhesive no	Fracture toughness (MN m ^{-3/2})
16	2.82
21	5.45

Close inspection of the crack surfaces after eventual failure shows no signs of crazing, indicating that the primary energy absorption mechanism in fatigue is shear yielding.

In contrast, adhesive 21 displays considerable whitening in the neighbourhood of the fatigue crack tip. This is indicative of crazing being the main energy absorption mechanism. Characteristically of crazed materials, the crack surfaces of the failed specimen show a rather blurred transition between the region of fatigue crack propagation and the region of fast fracture.

The superior fatigue performance of adhesive 16 is in contrast with the static fracture toughness, for which adhesive 21 is superior. This result is contrary to the trend discussed by Hertzberg and Manson²¹ who found that a high fatigue performance is usually indicative of a high fracture toughness. Nevertheless, they also found some examples of the anomalous behaviour described above.

It is interesting to speculate on a possible implication of this result. In the case of adhesive 16, fatigue crack propagation is associated with shear yielding close to the crack tip. The crack remains well defined throughout its gradual growth by fatigue, and sudden failure occurs when the static fracture toughness is eventually exceeded. In the case of adhesive 21, fatigue crack propagation is associated with multiple crazing close to the tip. Some of the minute cracks associated with this effect are encountered by the main fatigue crack, enabling it to grow more quickly than it otherwise would. However, the overall effect of the crazing is to extend the region of pseudo-plastic behaviour close to the crack tip, thereby blunting the tip and reducing the likelihood of static failure.

The authors accept that their two adhesives are insufficient by themselves to confirm the validity of this hypothesis. However, if it is indeed correct, future experiments should show a tendency for polymers exhibiting shear yielding to perform better in fatigue than

evidence deduced from static fracture tests would suggest. Conversely, materials exhibiting crazing would tend to perform more poorly in fatigue than might be expected from measurements of fracture toughness.

Quantitative results

The results of the fatigue tests on the two adhesives are presented in Figures 3–6 and Tables III–VI. By inspection, all the graphs are capable of interpretation as straight lines, thus showing that the Paris Law (Eq. (1)) represents the fatigue behaviour quite well provided that the frequency of load cycling remains constant. Each “graph” consists of many experimental points obtained from several specimens tested at different load ranges. Typically, about 30 data points are obtained with each specimen.

Figure 3 shows no particular trend as the frequency of cycling varies. The coefficient A_1 and the exponent B_1 in Eq. (1) are approximately constants even though the frequency ranges from 0.5 Hz to 5.0 Hz. The “frequency independent” values of A and B correlate very well with the overall data even though closer correlation can be achieved by treating each frequency independently. This is a useful feature of the adhesives from a designer’s point of view, but it is possible that a different result would be obtained at more extreme frequencies. At very low frequencies, creep influences the phenomenon; at very high frequencies, thermal effects can become significant.

Figure 4 shows that Eq. (2) is an equally good model of the crack growth in both adhesives, which implies that the material behaviour is approximately linearly elastic. Equations 3 and 6 are also found to be good models, but these are not shown graphically because no additional information is implied in the present experiments. This is because the stress ranges have not been varied.

Equation (5) gives a good approximation to the behaviour of adhesive 16, but it is not a good approximation for adhesive 21. The difference between the two cases lies in the method used to determine the fracture toughness (critical strain energy release, G_c). It is accepted that this method is inadequate for materials such as adhesive 21, and this implies that the fracture toughness should be deduced from a separate test. Happily, the need for this extra effort

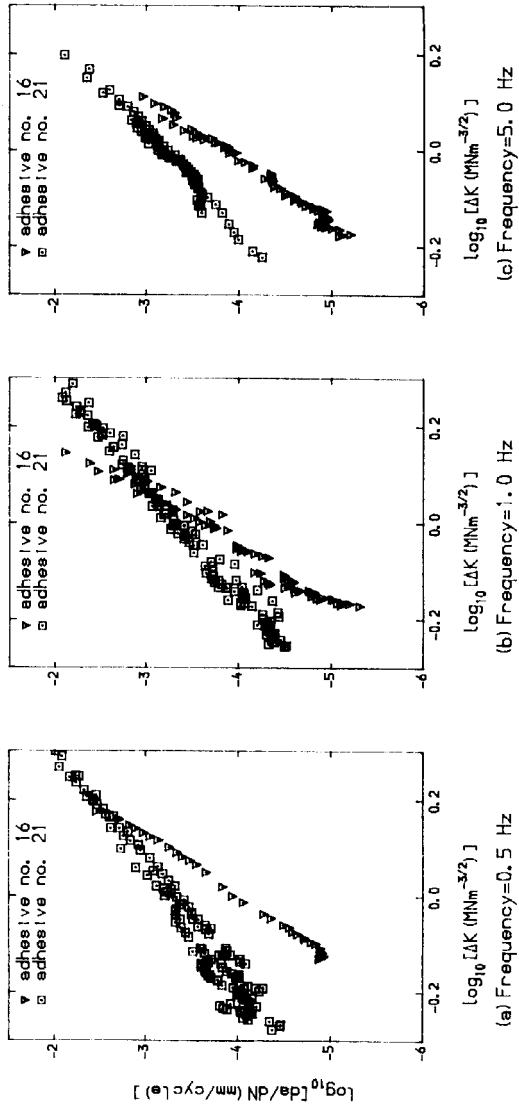


FIGURE 3 Representation of experimental results using Eq. (1).

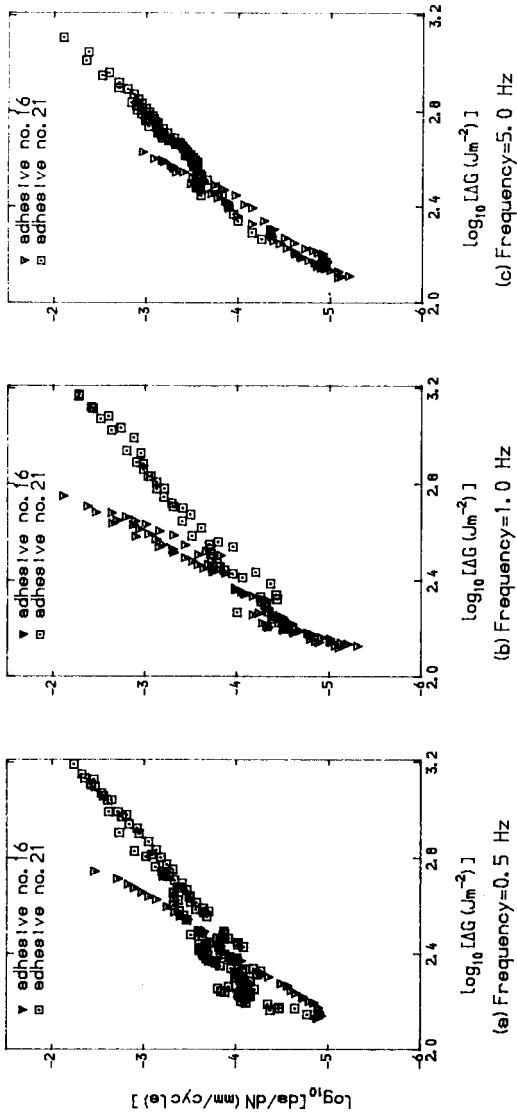


FIGURE 4 Representation of experimental results using Eq. (2).

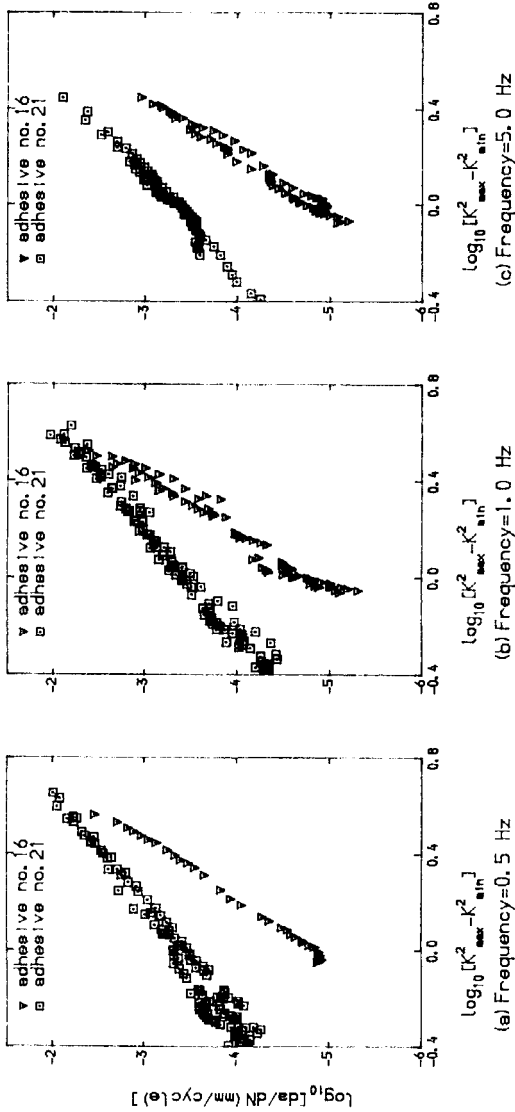


FIGURE 5 Representation of experimental results using Eq. (4).

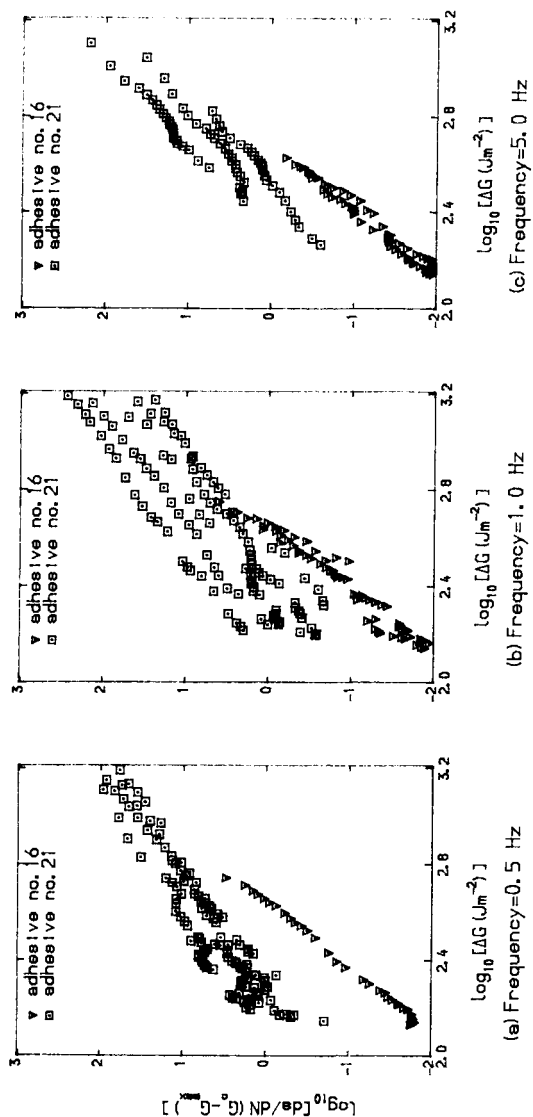


FIGURE 6 Representation of experimental results using Eq. (5).

TABLE III
 Constants A_1 and B_1 in Eq. (1)

Adhesive no	Frequency	A_1	B_1	Correlation coefficient (r)	Covariance (cov)
16	0.5	9.9243×10^{-5}	7.8114	0.9973	0.0825
	1.0	2.5674×10^{-4}	8.3681	0.9835	0.0756
	5.0	1.4145×10^{-4}	7.5741	0.9933	0.0518
	all	1.6807×10^{-4}	7.8101	0.9689	0.0686
21	0.5	5.7253×10^{-4}	3.9500	0.9772	0.1006
	1.0	4.6366×10^{-4}	4.5130	0.9915	0.1231
	5.0	6.5811×10^{-4}	4.7234	0.9871	0.0354
	all	5.4941×10^{-4}	4.2337	0.9787	0.0961

TABLE IV
 Constants A_2 and B_2 in Eq. (2)

Adhesive no	Frequency	A_2	B_2	Correlation coefficient (r)	Covariance (cov)
16	0.5	4.5467×10^{-14}	3.9029	0.9973	0.1652
	1.0	1.3198×10^{-14}	4.1790	0.9830	0.1511
	5.0	2.8840×10^{-14}	3.9922	0.9899	0.0976
	all	1.9702×10^{-14}	4.0796	0.9857	0.1359
21	0.5	2.5090×10^{-9}	1.9767	0.9781	0.2056
	1.0	3.5744×10^{-10}	2.2564	0.9915	0.2462
	5.0	2.6032×10^{-10}	2.3634	0.9872	0.0707
	all	1.0226×10^{-9}	2.1145	0.9789	0.1924
EC3445	3	1.81×10^{-14}	4.34		
FM300	3	1.52×10^{-15}	4.55		

TABLE V
 Constants A_4 and B_4 in Eq. (4)

Adhesive no	Frequency	A_4	B_4	Correlation coefficient (r)	Covariance (cov)
16	0.5	1.4713×10^{-5}	3.9032	0.9974	0.1652
	1.0	1.7077×10^{-5}	4.1801	0.9829	0.1511
	5.0	1.4635×10^{-5}	3.9904	0.9900	0.0977
	all	1.5492×10^{-5}	4.0794	0.9857	0.1359
21	0.5	4.4885×10^{-4}	1.9736	0.9775	0.2015
	1.0	3.5465×10^{-4}	2.2563	0.9915	0.2463
	5.0	4.9682×10^{-4}	2.3628	0.9871	0.0707
	all	4.2589×10^{-4}	2.1161	0.9789	0.1926

TABLE VI
 Constants A_5 and B_5 in Eq. (5)

Adhesive no	Frequency	A_5	B_5	Correlation coefficient (r)	Covariance (cov)
16	0.5	2.2264×10^{-10}	3.6439	0.9975	0.1542
	1.0	8.1809×10^{-11}	3.7961	0.9789	0.1366
	5.0	1.4348×10^{-10}	3.6573	0.9894	0.0896
	all	8.5035×10^{-11}	3.7813	0.9836	0.1259
21	0.5	6.1973×10^{-5}	1.9243	0.9544	0.1964
	1.0	7.4490×10^{-6}	2.2010	0.8879	0.2402
	5.0	1.7502×10^{-8}	3.1584	0.9090	0.0945
	all	2.0616×10^{-5}	2.0589	0.8843	0.1873

is not proven, however, because Eq. (5) does not appear to be superior to other equations, even for adhesive 16 (for which G_c can be deduced accurately).

Overall, adhesive 16 is most promising. The values of the constants A_2 and B_2 are similar to those reported by Mall and Johnson²⁴ for a thermosetting adhesive (EC3445) and a modified epoxy adhesive (FM300) at a frequency of 3 Hz—see Table III. The results are not directly comparable because they used a double-cantilever beam specimen, not a compact tension specimen, but the coefficients are sufficiently similar to give additional confidence in the two pieces of work. Adhesive 21 is far less resistant to fatigue than any of the other three adhesives, but it may nevertheless be suitable for many engineering applications where high frequency loads are of relatively small amplitude.

VI CONCLUSIONS

- 1) Fatigue tests on two toughened epoxy adhesives have shown that the rate of Stage II crack growth satisfies the Paris Law.
- 2) The single-part, hot-cure adhesive (number 16) performs better in fatigue than the two-part, cold-cure adhesive (number 21) even though the latter has a much greater fracture toughness.
- 3) Adhesive 16 shows no signs of crazing due to fatigue and, characteristically of materials that fail by shear yielding, it is highly resistant to crack initiation as well as to crack propagation.

4) Adhesive 21 shows clear signs of crazing around the crack tip and has a poorer resistance to crack initiation and propagation.

5) Both adhesives behave consistently and exhibit no dependence on the frequency of load cycling within the range 0.5 Hz to 5.0 Hz.

Acknowledgement

The authors wish to thank Permabond Adhesives Ltd and Ciba Geigy Plastics who supplied the adhesives free of charge.

References

1. R. R. N. Jones, J. Swamy, J. Bloxham and A. Bouderbalah, *Int. J. Cement Composites* **2**, 91–107 (1976).
2. M. D. Macdonald and A. J. J. Calder, *Int. J. of Adhesion and Adhesives* **2**, 119–127 (1982).
3. P. Albrecht, *Journal of Structural Engineering, ASCE* **113**, (1987).
4. D. M. Martin, Ph.D. Thesis, University of Dundee (1985).
5. R. J. Lark and G. C. Mays, WBRU Interim Report IR37, University of Dundee (May 1982).
6. R. J. Lark, WBRU Interim Report IR34 Rev. A, University of Dundee, (Nov 1983).
7. D. W. Hoepfner and W. E. Krupp, *Engineering Fracture Mechanics* **6**, 47–70 (1974).
8. P. C. Paris and F. A. Erdogan, *J. Basic. Engg. Trans. ASME, Ser. D* **85**, 528–534 (1963).
9. J. A. Marceau, J. C. McMillan and W. M. Scardino, *Proc. 2nd Nat. SAMPE Symposium and Exhibition*, San Diego, 64–80 (1977).
10. D. A. Jablonski, *J. Adhesion* **11**, 125–143 (1980).
11. W. D. Bascom and S. Mostovoy, *Am. Chem. Socy., Div. Org. Coat. Preprints*, Anaheim, California, 152–156 (1978).
12. J. M. Barsom, *ASTM STP 486* (American Society for Testing and Materials, 1971), pp. 1–15.
13. C. M. Radon, J. C. Arad and L. E. Culver, *Engineering Fracture Mechanics* **6**, 195–208 (1974).
14. C. M. Branco, J. C. Radon and L. E. Culver, *J. Strain Analysis* **12**, 71–80 (1977).
15. K. Tanaka, T. Hoshide and N. Sakai, *Engineering Fracture Mechanics* **19**, 805–824 (1984).
16. R. G. Forman, V. E. Kearney and R. M. Engle, *J. Basic Engg. Trans. ASME., Ser. D* **89**, 459 (1967).
17. S. J. Maddox, *Intern. J. of Fracture* **11**, 389–408 (1975).
18. W. Arad, J. C. Radon and L. E. Culver, *J. Mech. Eng. Science* **13**, 75–81 (1971).
19. C. W. Woo and C. L. Chow, *Intern. J. of Fracture* **26**, R37–R42, (1984).
20. Wolf Elber, *ASTM STP 486* (American Society for Testing and Materials, 1971), pp. 230–242.

21. R. W. Hertzberg and J. H. Manson, *Fatigue of engineering plastics* (Academic Press, NY, 1980).
22. ASTM E647, *ASTM Book of Standards*, ASTM Part **10**, 711–721 (1984).
23. J. Luckyram, W. J. Harvey and A. E. Vardy, *Proceedings thirteenth international symposium for testing and failure analysis*, Los Angeles, (Nov 1987).
24. S. Mall and W. S. Johnson, NASA Technical Memorandum 86355, (Feb 1985).